Chiang Mai J. Sci. 2020; 47(3) : 580-587
http://epg.science.cmu.ac.th/ejournal/
Contributed Paper

Visible and Ultraviolet Light Absorption of CuO-doped Fe Alloy Coatings Prepared by HVOF Thermal Spray Technique

Panupong Jaiban*[a], Pimpilai Wannasut [b] and Anucha Watcharapasorn [b,c]

[a] Faculty of Science, Energy and Environment, King Mongkut's University of Technology North Bangkok, Rayong Campus, Rayong 21120, Thailand.

[b] Department of Physics and Materials Science, Faculty of Science, Chiang Mai University, Chiang Mai 50200, Thailand.

[c] Center of Excellence in Materials Science and Technology, Materials Science Research Center, Faculty of Science, Chiang Mai University, Chiang Mai 50200, Thailand.

*Author for correspondence; e-mail: p.jaiban@gmail.com

Received: 21 March 2019
Revised: 6 November 2019
Accepted: 17 December 2019

ABSTRACT

Fe-based alloy coatings with CuO addition were prepared by HVOF and thermal absorption on visible and ultraviolet light of the prepared coatings was studied. The addition of CuO does not affect the crystal structure and microstructure of Fe-based coatings. The light absorption and the rate of the temperature increase are enhanced, leading to better conversion from photo to the thermal energy of CuO-doped coatings. The result here suggests the alternative property of Fe-based coatings, which may find future application for the visible and ultraviolet light absorber.

Keywords: UV light absorber, CuO-doped Fe coating, high-velocity oxygen fuel

1. INTRODUCTION

High-velocity oxygen fuel (HVOF) spraying is one of the widely-used technique for the industries due to the HVOF-prepared coating is denser, lower porosity, and stronger when compared with the others, i.e., plasma or flame spraying [1]. Among HVOF thermal sprayed coatings, the Fe-based alloy coating has played an essential role in the automotive parts such as hydraulic pistons, pump parts, and bearing. Moreover, the wear, erosion, and corrosion resistance of Fe-based coating have been focused extensively in several previous works [2, 3]. On the contrary, with these properties, the attention in thermal and optical properties of Fe-based coating is quite scarce.

Recently, the solar absorptance (α) of Ni-based alloy coating prepared by HVOF has been enhanced from 0.75 to 0.88, which makes this coating becomes an alternative material for solar absorber [4]. The solar absorber can convert from solar energy such as visible (VB) light to thermal energy through the light-absorbing ability of the material [5]. From the attractive finding in the Ni-based alloy coating, this therefore suggests the practical possibility of other thermal spray coatings for such application. As in the above mention, it is seen that Fe-based alloy coating has only been focused on mechanical properties. Interestingly, the thermal and optical properties of the coat-

ing have been emphasized rarely. Moreover, the solar thermal absorption of Fe-based coating has not been reported yet. Hence, we are, therefore, interested in studying such property of Fe-based coating prepared by the HVOF process. Several reports have revealed the enhancement in solar thermal absorption using the addition of CuO [6, 7]. Thus, in this work, Fe-based coatings are doped with CuO at various concentrations, and their thermal absorption on VB and ultraviolet (UV) light is discussed in detail.

2. MATERIAL AND METHODS

The starting materials were a commercial thermal spray-grade Fe-based alloy powder with particle size ~ 50 μm (H 420S; Dura-Metal) and CuO powder with particle size < 10 μm (≥99.95%; Sigma Aldrich). CuO powder was added in a content of x = 0, 1, 3, and 5 wt%. The Fe-based alloy and CuO powders were mixed within ethanol media and zirconia balls for 6 hrs. After drying, the mixed powder was sieved with a mesh number of 250 (opening size ~ 51 μm). The coatings were deposited for 5 mins onto low carbon steel plates in dimensions of 30 mm x 50 mm x 5 mm by Diamond Jet HVOF torch (Sulzer Metco) with the parameters as listed in Table 1. Before the process, the substrates were grit-blasted employing aluminum oxide to obtain a surface roughness.

Phase characteristic was studied by an X-ray diffractometer (XRD). A scanning electron microscopy (SEM) in the backscattering electron (BSE) mode was used to observe the microstructure. For thermal absorption of the coatings, the samples were irradiated by VB light from a tungsten-halogen lamp (reflecta 8002, 400-800 nm) and UV light (405 nm) (see in Figure 4(a)). The edge and bottom of the samples were connected to a commercial polyethylene (PE) foam with a thickness of 10 mm; meanwhile, its top side was connected to a transparent mirror with a thickness of 4 mm. This setup was carried out to prevent thermal loss of all samples from two factors including thermal conduction and thermal convection. Besides, the bottom side of the PE foam was drilled to make a hole having a diameter that the sample could exchange the heat with another medium i.e., air atmosphere in this case. The area of light exposure was confined in an area having a dimension of 30 mm x 50 mm, which is equal to the sample size. A thermal camera (THT70) was used to detect their temperature variation upon light exposure. The absorptance spectrum of all coatings was measured by UV-visible spectroscopy (Shimadzu, UV-2600)

3. RESULTS AND DISCUSSION

X-ray diffraction (XRD) patterns of all powders are shown in Figure 1(a). Regarding the Fe powder, the material shows a ferrite phase with a cubic structure, which corresponds to JCPDS standard number 006-0696. Interestingly, the small peak at $2\theta \sim 40^{o}$ was present when CuO is added. This peak is related to the copper oxide phase (JCPDS # 80-0076), which suggests the composite powder between Fe and CuO phases. Figure 1(b) presents XRD patterns of all thermally

Table 1. Process parameters for the Diamond Jet HVOF torch.

Air flow rate (L/min)	410
O_2 flow rate (L/min)	273
Fuel flow rate (L/min)	40
Powder feed rate (g/min)	60
Spray distance (mm)	300

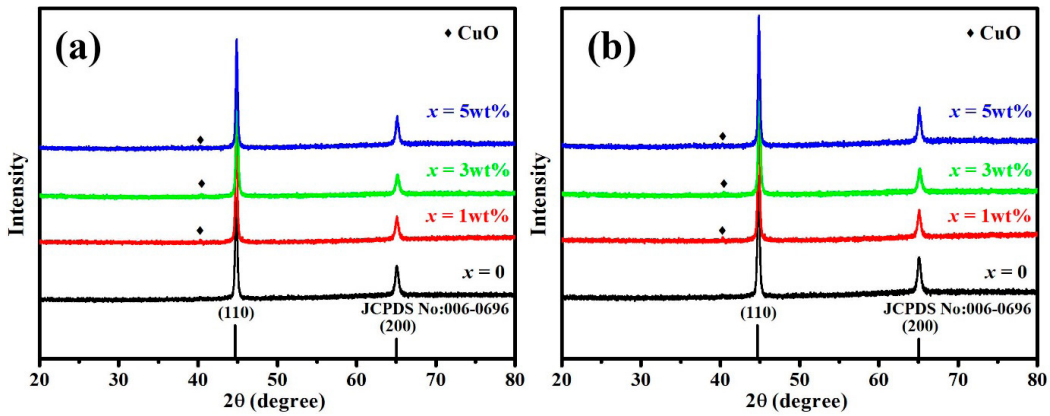

Figure 1. XRD patterns of all powder (a) and coatings (b).

sprayed coatings. XRD patterns of all coatings are ferrite phases with cubic structure, similar to those of their respective powders. Besides, the small peak of the CuO phase is also observed in the modified coating. The results indicate that HVOF technique does not result in their crystal structure transformation, i.e., both powder and coatings possess a ferrite phase with cubic structure. However, upon thermal sprayed process at high temperature, the powder can react with the oxygen in air atmosphere and produces the additional phase in the coatings, which would be discussed in later section.

The BSE images of all coatings are illustrated in Figure 2. The thickness of all coatings is about 250 μm. The microstructural feature, including a few pores, splat layers, and incompletely melted particles, can be observed clearly in all coatings.

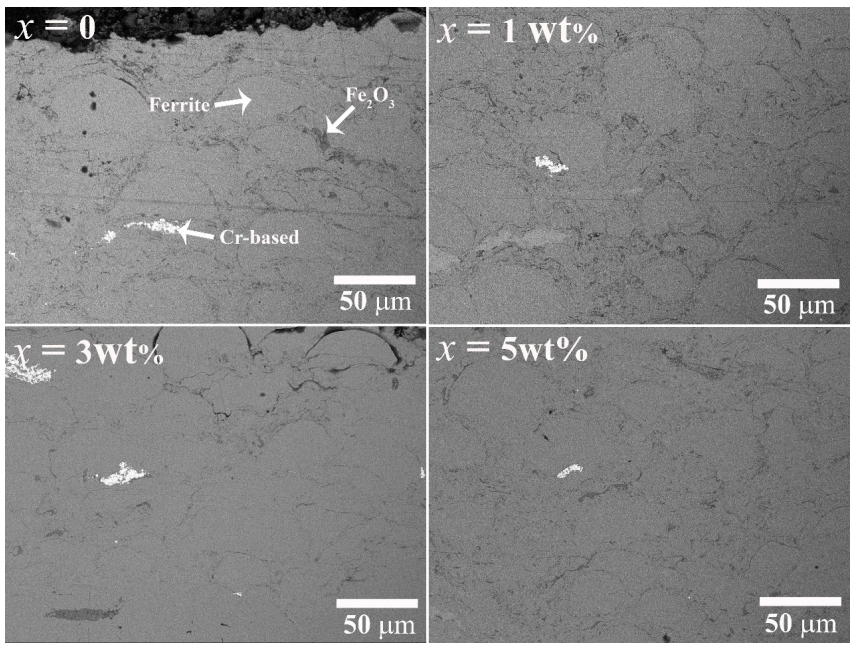

Figure 2. BSE images of Fe-based coatings with different CuO content.

The dense microstructure indicates that the CuO addition does not influence the fabrication of Fe-based coatings by the HVOF technique. In the case of the splat layers, it attributes to the complete fusion of particles and deposition on the substrate, forming the splat-like layer. For the partially melted particles (i.e., having the sphere or semicircle shape), they are often present during the thermal spray process, which reflects that the lacking period of some particles flying in the flame spray [8]. According to the BSE images of all coatings, it is seen that all coatings are composed mainly of the gray area, which is the ferrite phase. This observation corresponds well with the energy-dispersive X-ray spectroscopy (EDS) of this area as shown in Figure 3 and the observed elements listed in Table 2. This area has maximum Fe concentration. Thus, this should be the ferrite phase. Moreover, the observed elements of such area and the pure powder are associated with each other. Interestingly, the additional phases (i.e., dark and white areas) are revealed by BSE images of all coatings. The EDS analysis is, therefore, used to determine such phases of the representative samples, i.e., the coating with x = 0.3wt%. The EDS results of the selected samples are shown in Figure 3 and the quantitative data of observed elements for each area are listed in Table 2. From the results, it is seen that the other phases are chromium (Cr)-rich phase (white color) and iron oxide (Fe_2O_3; dark color). Since the Cr is doped to increase the corrosion resistance of the commercial Fe powder, the Cr-rich phase is observed in the coating. This is confirmed by the observation of Cr in pure powder as shown in Figure 3 and Table 2. In the case of Fe_2O_3, it is the fact that Fe particles react with oxygen in the atmosphere during the thermal spray process and form the iron oxide phase [9].

The experimental setups for the temperature variation of all coatings upon VB and UV light exposure are illustrated in Figure 4(a). The contribution of the substrate is also taken into account to obtain the actual response of the coatings. The relationship of the exposure time upon VB light and the temperature difference (ΔT) between the initial and variated temperatures is shown in Figure 4(b). The temperature of all samples increases rapidly in the first period of 5 min and becomes much slower with more extended time. Then, the temperature seems to be stable after 25 min. This result may suggest the saturation of all coatings upon the VB light irradiation. The increase of the coating temperature during VB light exposure can be explained by the contribution from the conversion of photon energy to thermal energy, which is a general feature of the solar absorber material [5]. The pure coating shows a similar temperature evolution to that of substrate, where the maximum value of ΔT is about 30 ^{o}C at 30 min. Interestingly, the thermal absorption of the coatings is improved when CuO is added. The maximum ΔT is approximate 32.5 ^{o}C, and 37.5 ^{o}C for the concentration of 1 wt% and higher, respectively. There are two possible reasons for this enhancement. For the first one, the increase in solar absorption of Fe-based coatings results from the addition of CuO due to the fact this material has high solar absorption, as suggested by several reports [6, 7]. For second reason, it may be attributed to the presence of Fe_2O_3 within all coatings. This iron oxide has promoted enhanced light absorption in several reports [10, 11]. Thus, the amount of Fe_2O_3 for each coating, therefore, is analyzed using ImageJ software [12]. The results of all coatings are shown in Figure 5. As seen in the figure, the red area indicating the quantity of Fe_2O_3 increases slightly with increasing of CuO. This may be an additional reason for better solar absorption of the coating with CuO addition above 1 wt%. However, this hypothesis would still need a further experiment and investigation relating to influence of Fe_2O_3 amount on solar absorption of these coatings.

The UV light is irradiated on all coatings and the substrate, and the plot of ΔT and the exposure time is shown in Figure 4(c). The increases of ΔT is abrupt in the first period of

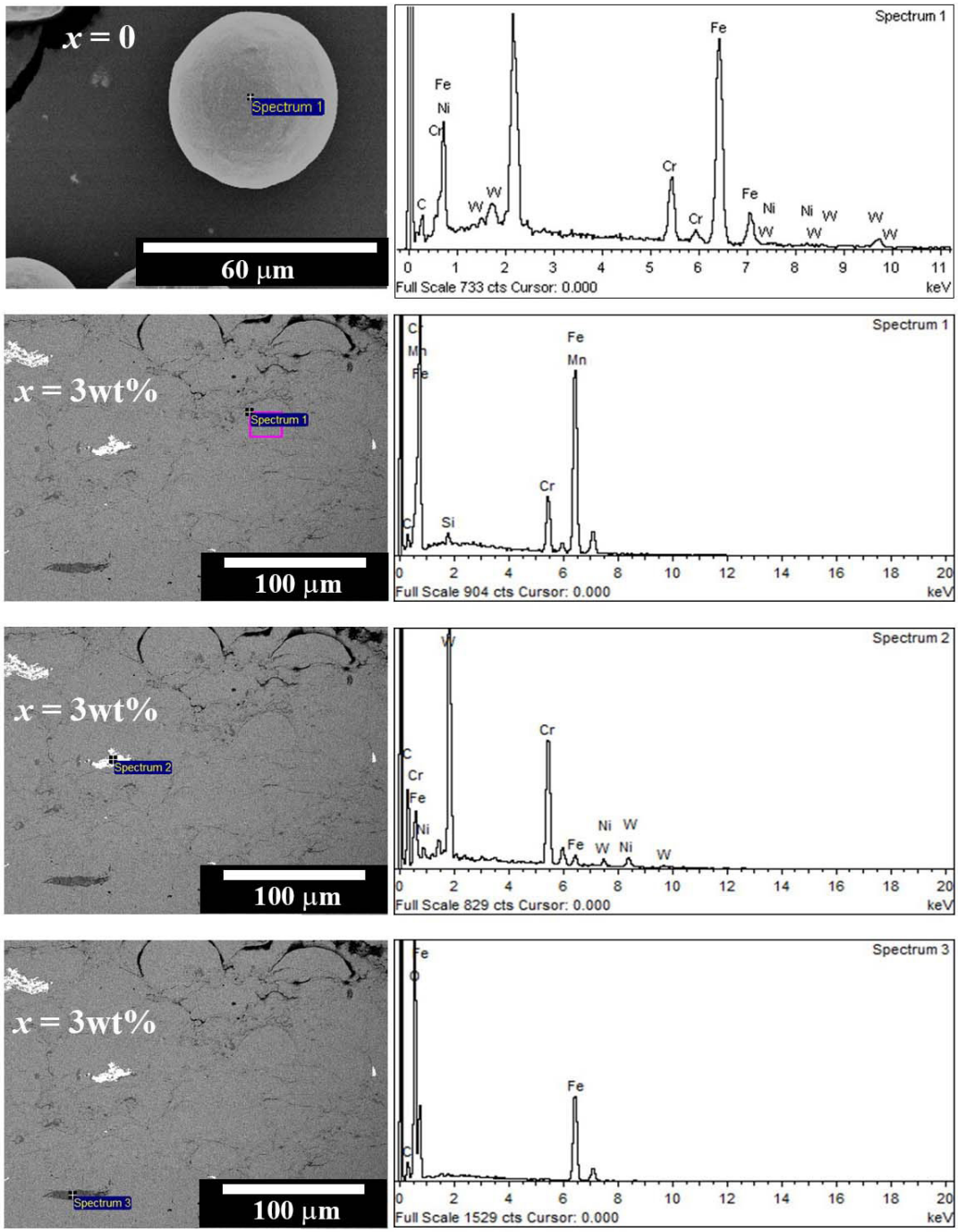

Figure 3. EDS results of the selected samples.

Table 2. Chemical analysis of the powder ($x = 0$), and the coating (x=3 wt%).

Elements (atomic %)	Powder	Gray area	White area	Dark area
C	23.87	23.23	25.62	14.83
Cr	11.49	11.23	61.01	-
Fe	64.22	63.09	2.85	29.17
Ni	0.40	-	2.21	-
W	0.02	-	8.31	-
Si	-	1.34	-	-
Mn	-	1.11	-	-
O	-	-	-	56.00
Total	100.00	100.00	100.00	100.00

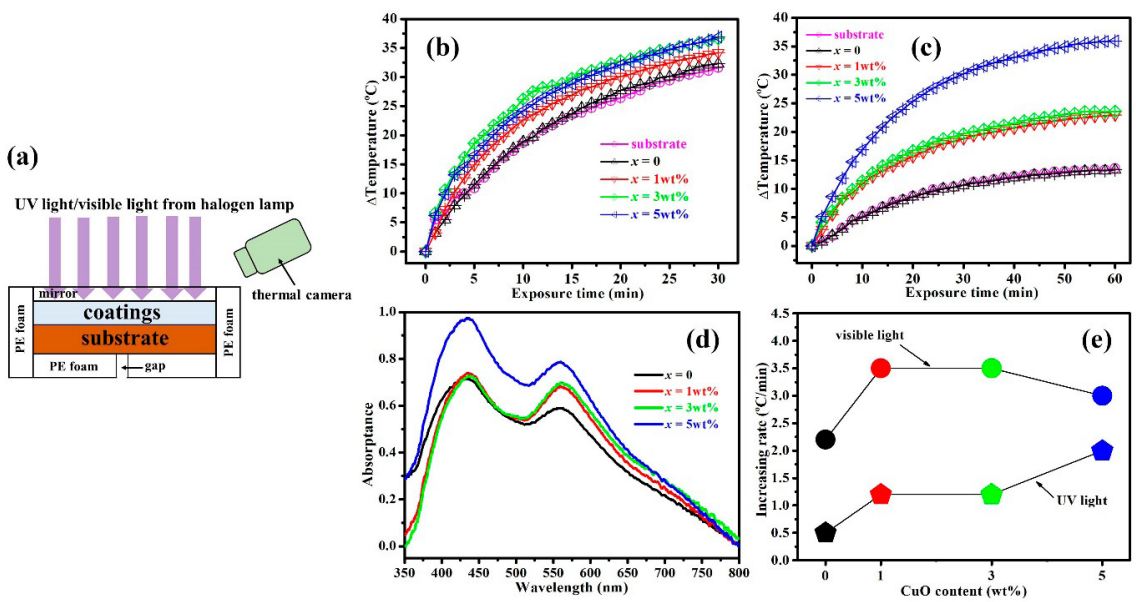

Figure 4. Experimental setup (a), ΔT as a function of exposure time of all coatings under VB (b) and UV light (c), absorptance of all coatings (d), the increasing rate of the temperature at 5 mins of all coatings (e).

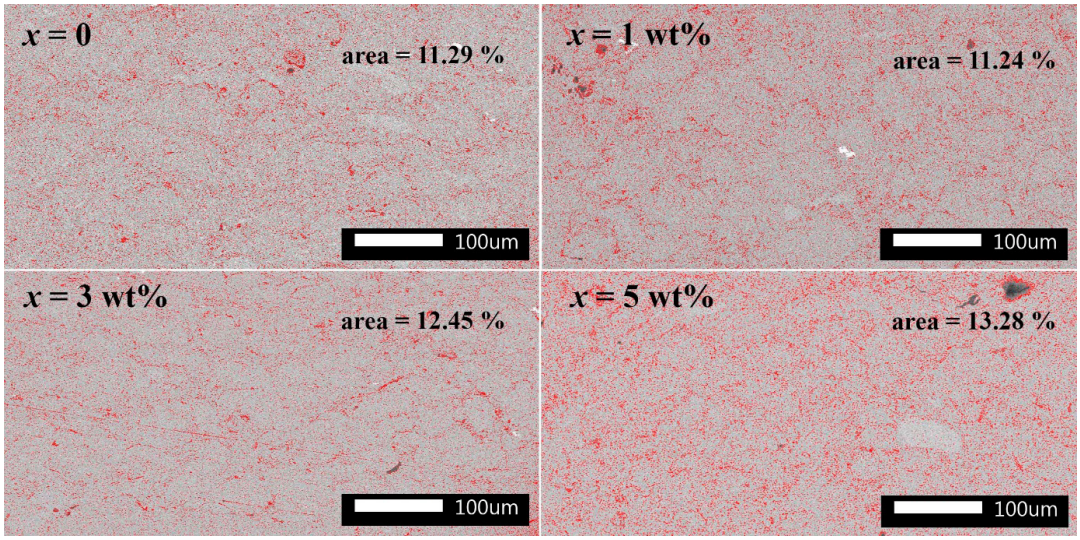

Figure 5. Image analysis of Fe_2O_3 of all coatings.

10 min and becomes slower when the time passes up to 50 min, then the value becomes stable. This result may suggest the saturation point of these materials on UV light irradiation. The increase of the coating temperature upon UV light can be explained by the phenomena similar to that of VB light. There is no significant difference in UV light for the pure coating and the substrate. However, the CuO-doped coatings promote the better absorption of UV light when CuO increases, particularly at 5 wt%. The maximum ΔT is about 35 °C at 60 min, which is much better than the pure coating (ΔT ~ 10 °C at the same exposure time). This result indicates the significant enhancement in UV light absorption of Fe-based coatings via CuO addition.

Figure 4(d) shows the spectra of the light absorptance of all coatings in the range of wavelength from 350 to 800 nm, which covers UV light (405 nm) and VB light (400 to 800 nm). It is evident that the Fe coating with CuO at 5 wt% exhibits the significant absorption (~0.9 – 1) in UV light wavelength (~400 - 450 nm), resulting in the substantial ΔT value of this material (see in Figure 4(c)). The large UV light absorption of the coating at 5 wt% may be attributed to the amount of Fe_2O_3 observed in Figure 5. This is associated with the absorption spectrum at 400 - 500 nm wavelength of Fe_2O_3 reported in previous work [11]. In the case of the absorption spectrum in 500 – 800 nm range of all coatings, the absorptance is not much different (~0.6 – 0.8). This result, therefore, causes the slight difference of ΔT value of all coatings observed in Figure 4(b).

The rate of the temperature increase at 5 min upon VB and UV light exposure of all coatings are summarized in Figure 4(e). The pure coating shows the increasing rate of about 2 °C/min while the CuO-doped coatings show a higher value ~3.0 - 3.5 °C/min for VB light irradiation. Similarly, the addition induces the higher rate of the temperature increment upon UV light in CuO-doped coatings (~1.3 - 2.0 °C/min) when compared with the pure coating (~0.5 °C/min), indicating that CuO addition not only induces the better light absorption but also causes the more active response of Fe-based coatings on VB and UV light stimulus.

4. Conclusions

The CuO addition does not affect the crystal structure and microstructure of Fe-based coatings

prepared by the HVOF technique. The dopant enhances VB and UV light absorption and the rate of the temperature increase, leading to the better conversion of a photon to thermal energy. The light-to-thermal energy conversion of Fe-based coatings becomes more efficient at 5wt% CuO addition. The results in this study show that the thermally sprayed CuO-added Fe-based coatings could be useful and may find future application as a VB and UV light absorber.

ACKNOWLEDGMENTS

This research was funded by the King Mongkut's University of Technology North Bangkok. Contract no. KMUTNB-63-KNOW-011.

REFERENCES

[1] Herman H., Sampath S. and McCune R., *MRS. Bull.*, 2005; **25**: 17-25. DOI 10.1557/mrs2000.119

[2] Bolelli G., Bonferroni B., Laurila J., Lusvarghi L., Milanti A., Niemi K. and Vuoristo P., *Wear*, 2012; **276**: 29-47. DOI 10.1016/j.wear.2011.12.001

[3] Qiao L., Wu Y., Hong S., Qin Y., Shi W. and Li G., *J. Mater. Eng. Perform.*, 2017; **26**: 3813-3820. DOI 10.1007/s11665-017-2590-1.

[4] Cao Y., Xiong J., Gong D., Li J. and Ding M., *Vacuum*, 2015; **121**: 64-69. DOI 10.1016/j.vacuum.2015.07.018.

[5] Amri A., Jiang Z.T., Pryor T., Yin C.Y. and Djordjevic S., *Renew. Sust. Energ. Rev.*, 2014; **36**: 316-328. DOI 10.1016/j.rser.2014.04.062.

[6] Malliga T.V. and Rajaseknar R.V.J., *J. Therm. Anal. Calorim.*, 2017; **129**: 233-240. DOI 10.1007/s10973-017-6155-1.

[7] Arunkumar T., Murugesan D., Raj K., Denkenberger D., Viswanathan C., Rufuss D.D.W. and Velraj R., *Appl. Therm. Eng.*, 2019; **148**: 1416-1424. DOI 10.1016/j.applthermaleng.2018.10.129.

[8] Limpichaipanit A., Banjongprasert C., Jaiban P. and Jiansirisomboon S., *J. Therm. Spray Technol.*, 2013; **22**: 18-26. DOI 10.1007/s11666-012-9844-0.

[9] Limpichaipanit A., Wirojanupatump S. and Jiansirisomboon S., *Surf. Coat. Technol.*, 2015; **272**: 96-101. DOI 10.1016/j.surfcoat.2015.04.018.

[10] Wu S., Cheng C.H., Hsiao Y.J., Juang R.C. and Wen W.F., *Renew. Sus. Energ. Rev.*, 2016; **58**: 574-580. DOI 10.1016/j.rser.2015.12.263.

[11] Shinde S.S., Bansode R.A., Bhosale C.H. and Rajpure K.Y., *J. Semicond.*, 2011: **32**: 1-8. DOI 10.1088/1674-4926/32/1/013001.

[12] Schneider C.A., Rasband W.S. and Eliceiri K.W., *Nat. Methods.*, 2012; **9**: 671-675. DOI 10.1038/nmeth.2089.